# Preparation and detection of reconstructed plan-view surfaces

D.N. Dunn, R. Ai, T.S. Savage, J.P. Zhang and L.D. Marks

*Department of Materials Science and Engineering, Northwestern University, Evanston, IL 60208, USA*

It is shown that ion-beam thinning and cleaning of bulk single-crystal samples coupled with annealing can produce surfaces suitable for conventional plan-view imaging including HREM. The key elements are to ensure the absolute cleanliness of the sample preparation system, care in choosing proper ion beam energies, and choosing the appropriate annealing conditions so as to minimize coarsening by bulk diffusion. The presence of surface reconstructions can be readily detected in off-zone diffraction patterns and in on-zone two-beam bright- and dark-field images.

## 1. Introduction

Whereas the basic techniques for obtaining surface-sensitive images in an electron microscope are now fairly well established [1–14], a critical limitation has been the problem of producing samples of a quality comparable to those produced routinely for conventional bulk microscopy. This is most clearly seen by the fact that most microscopy sample surfaces produced in a fairly clean fashion thus far have been prepared by either heating or evaporation. While heating is known to work for silicon, it cannot in general be used for other materials. Evaporation has been used in the past for gold samples, but it cannot produce specimens free of artifacts from substrate materials nor can it produce large, single crystals. The most common method of producing clean surfaces for ultrahigh-vacuum (UHV) surface science experiments is a combination of mechanical polishing, ion beam sputtering and annealing. The question one must address is whether the same process can be used to produce microscope-grade surfaces.

The intention of this note is to demonstrate that clean surfaces of bulk single crystals can be prepared by standard mechanical and/or chemical polishing, ion beam sputtering and annealing treatments. This process of specimen preparation can then be monitored both for the presence of a reconstructed surface and for impurities by standard electron microscopy techniques. In the following sections we will briefly describe the general experimental approach, then focus on some of the more critical experimental issues and finally, discuss the observation of reconstructed surfaces.

## 2. Experimental equipment

All the experiments described here were performed in a Hitachi UHV-H9000 microscope, which is shown schematically in fig. 1. The microscope is a conventional HREM redesigned to achieve an ultimate pressure of about $6 \times 10^{-11}$ Torr in the specimen region, with differential pumping of the regions above and below the specimen, and is bakeable to 200°C. The operating vacuum is $1–3 \times 10^{-10}$ Torr which is stable for at least 6 months. The system can then be baked and returned to UHV conditions with a total turn-around time of 2–3 days at most. Attached to the microscope is a specimen transfer chamber (STC) equipped with a number of different instruments which can be changed at will. There are three particularly important accessories for the work described herein, namely a
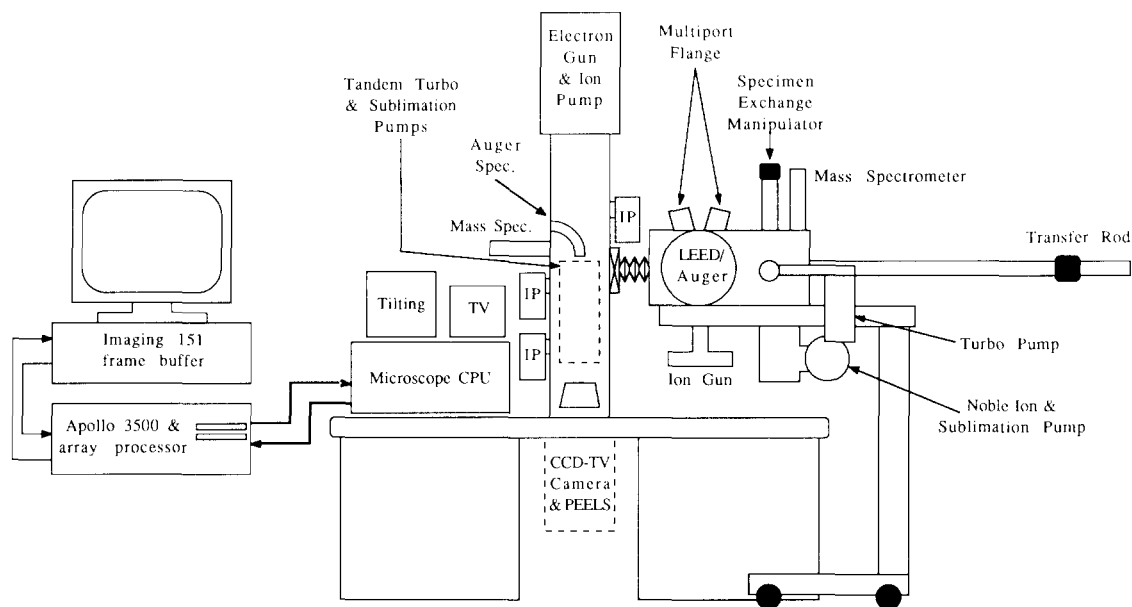
Fig. 1. A schematic diagram of the Hitachi UHV-H9000 and UHV-STC (courtesy of John Bonevich).

1–10 keV electron gun capable of delivering 3 mA of current into a 1 mm spot, a broad-band optical annealing source focussed onto the specimen by an external lens system, and a differentially pumped ion gun which operates in an energy range from 100 eV to 4 keV with neon, argon or xenon sources. The STC is separately pumped by a 60 ℓ/s ion pump with an attached titanium sublimation pump and is rough-pumped by a 50 ℓ/s turbomolecular pump.

Before proceeding any further, some important points should be made about the cleanliness requirements for the STC during ion milling and annealing of the specimen. We have found that the important thing to monitor is the hydrocarbon background of the vacuum, not the overall vacuum level. In particular, the level of hydrocarbon contamination should be monitored particularly when the sample is heated or during ion beam sputtering. The reason is that it is possible to achieve a base pressure with a reasonable-looking residual gas spectrum, but as soon as the chamber is heated during annealing or the sample is being ion beam sputtered, the hydrocarbon background can change substantially. It is quite often the case that significant hydrocarbon contamination is present on the walls of the chamber which are not detected by RGAs until they desorb when the walls are heated, by collision with sputtering gases or secondary electrons. For example, when ion beam sputtering with Xe, unless the hydrocarbon background was $< 10^{-9}$ Torr with a Xe pressure of $10^{-6}$ Torr, the surfaces were contaminated with carbon–the ion beam was cracking the vapor-phase hydrocarbons. This problem can be overcome by baking the transfer chamber for 2–3 days into the ion pump in order to clean the chamber walls. Another precaution

Fig. 2. A montage of images of a single-crystal Au(001) at various stages in the surface preparation process. (a) Bright-field image of the specimen just after thinning with 4 keV Xe ions. The fringes seen are moiré fringes caused by the ordered implantation of Xe on the Au lattice. (b) Dark-field image of the same sample seen in (a) after annealing. The Xe concentration has disappeared and dislocations are present. (c) A dark-field image taken with the (200) and surface spots shows the same sample after further annealing. Of note in this picture are the square holes and voids remanent from the ion beam sputtering process. The square holes in the sample indicate that ordering of the hole surfaces has taken place. This sample is suitable for study and in fact shows moiré fringes from the "5" dimension of the $5 \times n$ reconstructed unit cell.
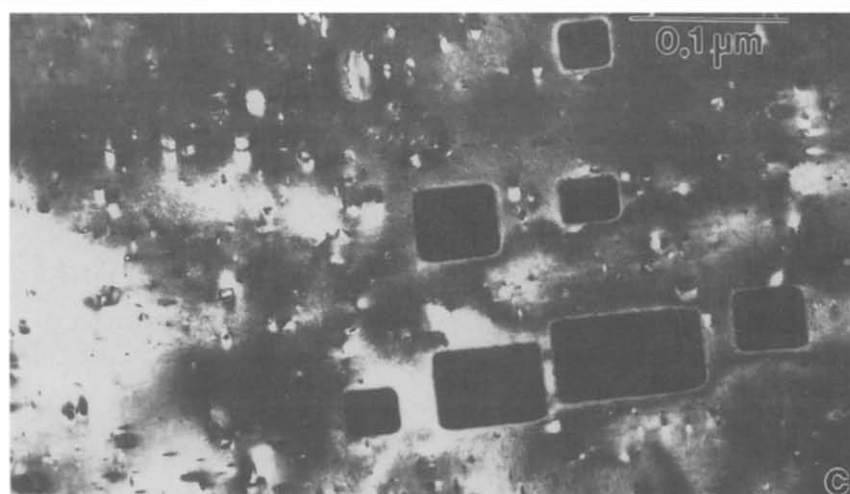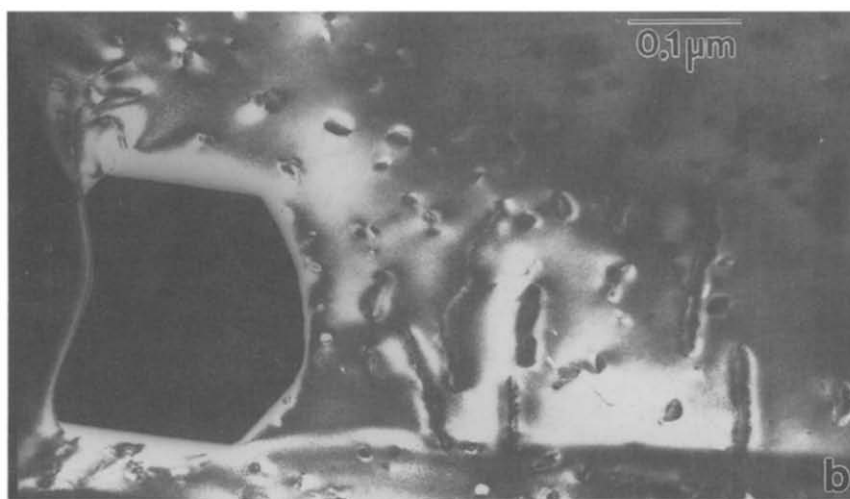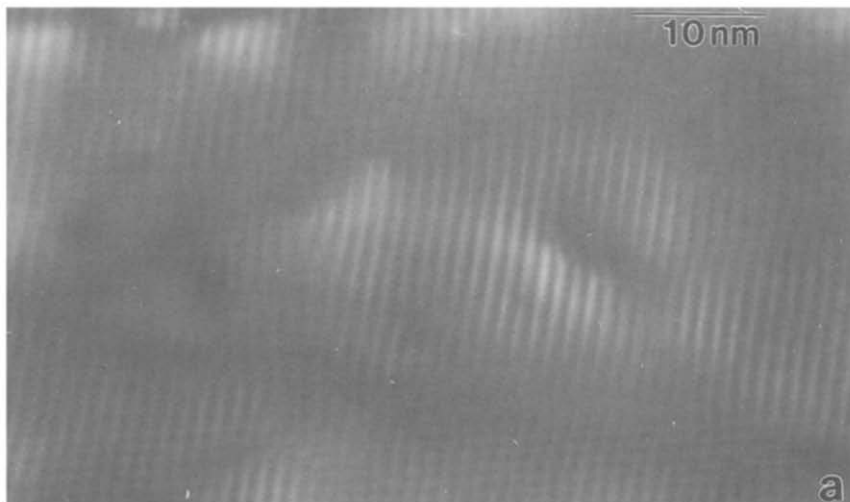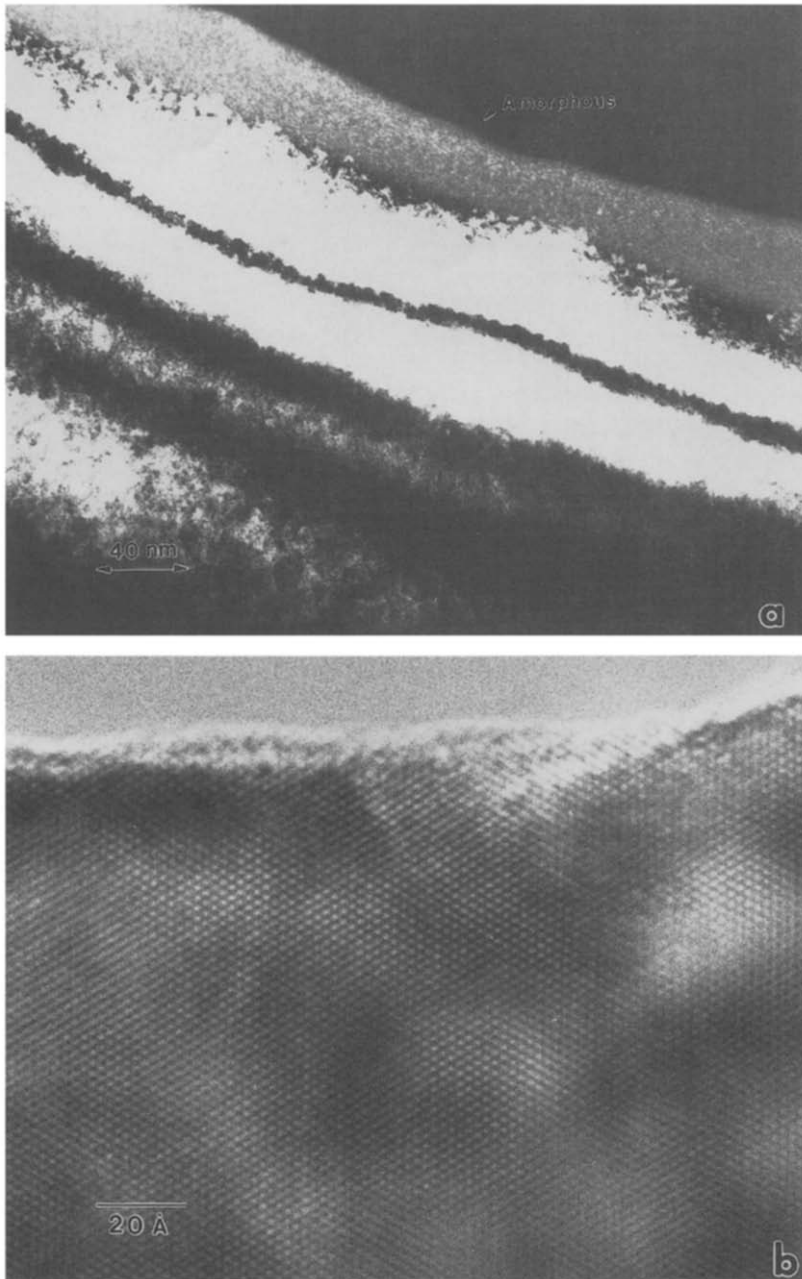
Fig. 3. (a) Bright-field image of a Si(111) single-crystal sample after initial thinning with 3 keV Xe ions. An amorphous layer near the surface can be seen which resulted from the ion thinning. This layer can be taken care of by further ion beam sputtering and annealing. (b) High-resolution image of the same sample after annealing. The amorphous layer is gone and the sample is relatively defect-free.

that can be taken to avoid contamination is to use the clean tandem-turbo pump on the microscope to pump the inert gas during ion beam sputtering instead of the ion pump on the STC. This will reduce the amount of time sputtering gases are present in the STC, minimizes hydrocarbon release by sputtering in the ion pump and avoids swamping the ion pump with noble gases. A related point is that it is critical to avoid exposure of the sample to contaminants from any of the instrumentation during any degassing. It should be appreciated that the above precautions are well known in surface science, but also place stringent restrictions on the design of UHV electron microscopes.

## 3. Initial sample preparation

We should briefly mention the initial stages of sample preparation that we have used. Both the gold (001) and silicon (111) samples used in this study were bulk single crystals which were mechanically polished and then dimpled. The gold samples were then ion milled from one side until fairly thin ($\sim$ 1000 nm), loaded into the transfer chamber and thinned with 4 keV Xe until there was a small perforation. The mechanical polishing of the gold led to some recrystallization, and it is hoped to avoid this in the future. The silicon samples were chemically polished from one side with a 10%-HF $HNO_3$ solution until there was a small hole and then moved into the STC. Our experience is that the starting sample must be clean and fairly electron-transparent for the best results.

## 4. Surface preparation

The preparation of surface-science-grade microscopy specimens involves two major steps. The first step is the bulk thinning process described in the previous section. The second stage is the preparation of the surface which is done exclusively in the STC by an iterative application of ion beam sputtering and annealing. The evolution of the surface is concurrently monitored for cleanliness and reconstruction by conventional microscopy and parallel electron energy loss spectroscopy (PEELS).

The use of ion beam sputtering and annealing to successfully produce a surface-science-grade microscope specimen raises the following concerns:

(a) Ion beam sputtering and mixing of the specimen holder or any support films with the specimen.

(b) Introducing bulk defects and implanting ions and surface contaminants during the ion beam sputtering process.

(c) Heating to temperatures sufficiently high and for long enough to anneal out most of the bulk defects.

(d) Avoiding annealing at too high a temperature or for too long because either of these may cause the sample to coarsen and become too thick for electron microscopy.

The first two problems are to a large extent mutually exclusive. Bulk defects can be avoided by sputtering at small angles or with lower-energy ions, but this increases the danger of sputtering the support. Our solution has been to use self-supporting 3 mm specimens, limit the ion beam energy to 1–3 keV (when the beam can be focussed to 1 mm) and limit the angle of incidence to $90 \pm 20°$. This incidence angle is admittedly
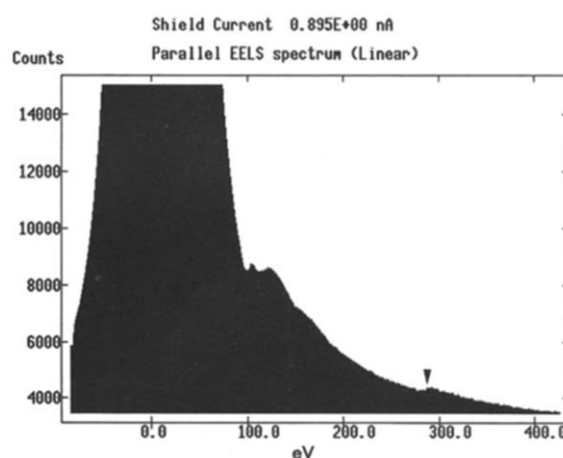


Fig. 4. PEELS spectrum from a boron-doped Si(111) single crystal showing initial silicon carbide formation contaminating the surface.

harsh and undoubtedly leads to defect production which could be alleviated by reducing the angle of incidence. A specimen-holder design is currently being tested which allows for smaller angles of incidence without sputtering the specimen holder. We have found it necessary to use energies of 2 keV or more in order to remove the initial partially graphitic carbon layer on the surface. (These layers come from the initial air exposure of the sample coupled with the cracking of residual hydrocarbons from pump oils and other systemic contaminants during the bake.) The optimum condition in our current setup is an ion energy of 1–2 keV, which at least for Xe does not appear to lead to substantial implantation and limits the damage to the near-surface region.

The next issue is to avoid substantial bulk diffusion and coarsening during annealing, but activate sufficient surface diffusion to order the surface. For each material the details of the procedure will be different, but we have found that one can produce HREM thin regions with care.

To illustrate the above points, figs. 2 and 3 show a montage of images during the preparation process. Fig. 2 is for a gold (001) sample and shows (a) a sample implanted with Xe, in (b) the same sample after optically annealing showing the removal of the implanted Xe, and in (c) the sample in (b) re-sputtered and optically annealed. The sample in (c) is suitable for study. Fig. 3 shows a silicon (111) sample after initial sputtering with the 3 keV Xe with an amorphous surface layer and in (b) a high-resolution image after electron beam annealing. More details of the specific results will be presented elsewhere [15,16].
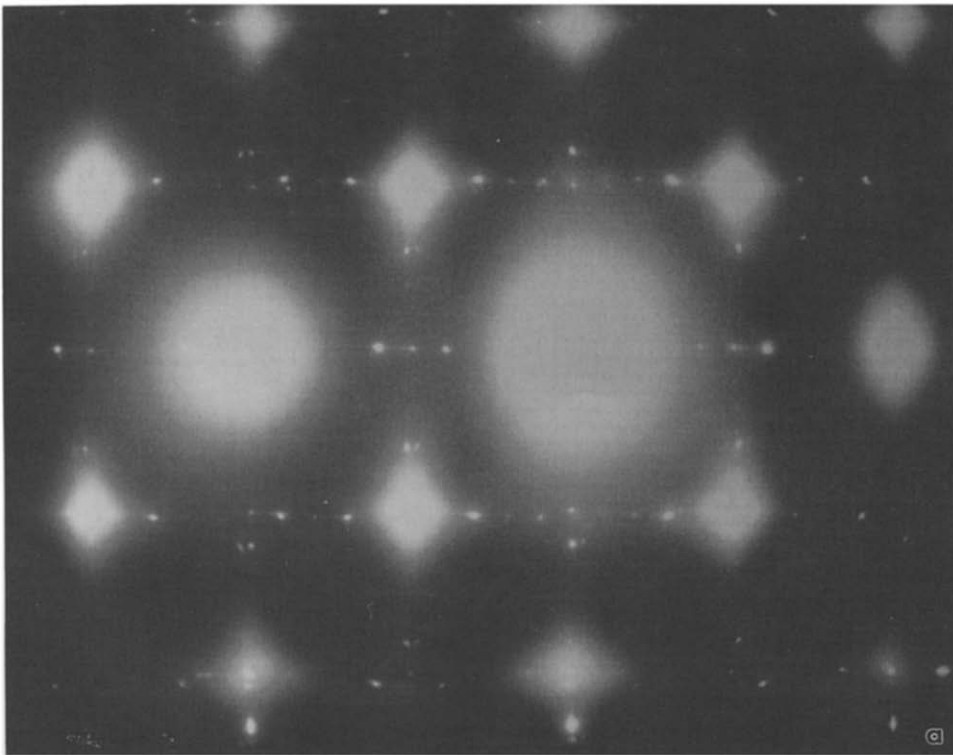


Fig. 5. (a) Diffraction pattern from boron-doped Si(111) 7×7 surface with co-existing silicon carbide – see also fig. 6c. (b) Off-axis diffraction pattern of the Au(001) 5×n reconstruction.

## 5. Monitoring the surface

It is clearly important to be able to monitor the surface, detect impurities and defects and the existence of surface reconstructions. While bulk defects can be readily imaged, surface contaminants are more problematic. Carbon, one of the most common contaminants, can be imaged in bright field or detected by PEELS as is seen in fig. 4. Our best estimate of the PEELS sensitivity is several monolayers; images appear to be more sensitive particularly to carbon on the surface, particularly in profile.

The detection of surface reconstructions is best done by a two-pronged approach which involves diffraction patterns and conventional TEM imaging techniques. Diffraction patterns in on- and off-zone configurations contain all the necessary information for determining the type and symmetry of reconstructed domains. Off-zone diffraction patterns have a better ratio of surface-to-bulk spot intensity which makes the surface spots more clearly visible. In addition, off the zone axis the effects due to phonons and plasmons around the bulk reciprocal lattice vectors are damped and the contrast (not the intensity) of the weaker surface spots is greater. As an example of this, Fig. 5a shows a tilted diffraction pattern from the Au(100) $5 \times n$ reconstruction and Fig. 5b a diffraction pattern of the metastable boron-doped Si(111) $7 \times 7$ reconstuction in the presence of some silicon carbide, near the zone axis.

The imaging techniques we have found to be most useful are bright- and dark-field images as well as two-beam and weak-beam images. Dark-field images taken with the bulk and surface spots give complementary information to that of the diffraction patterns and show the morphology of
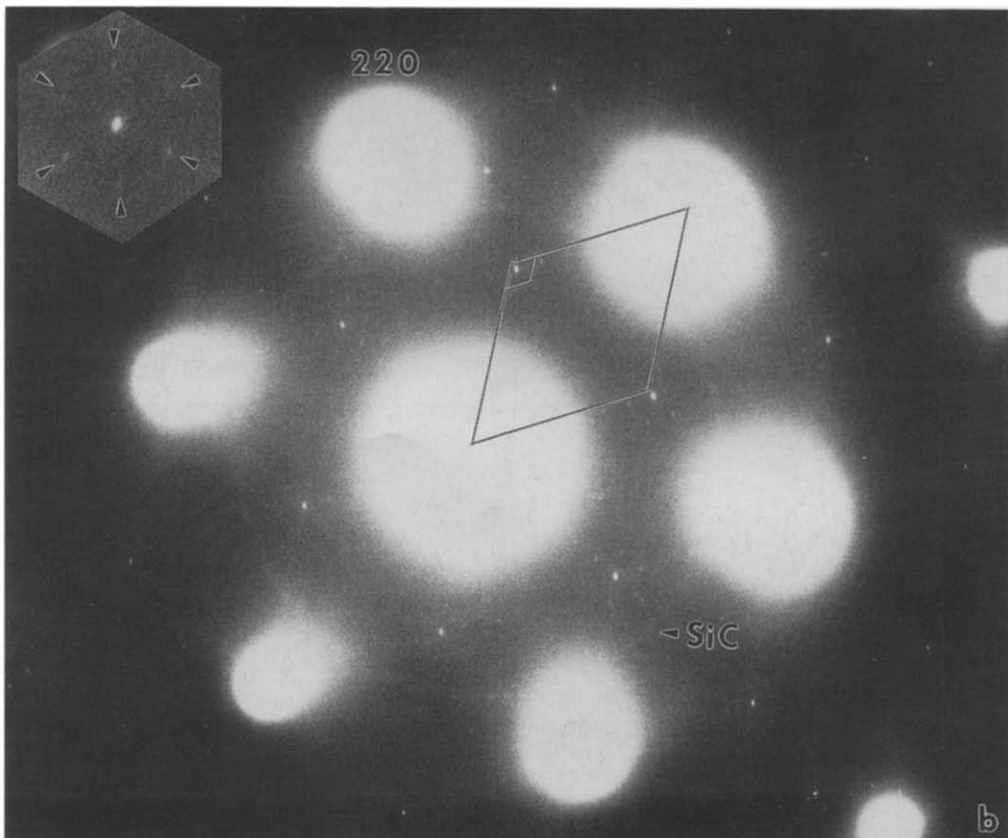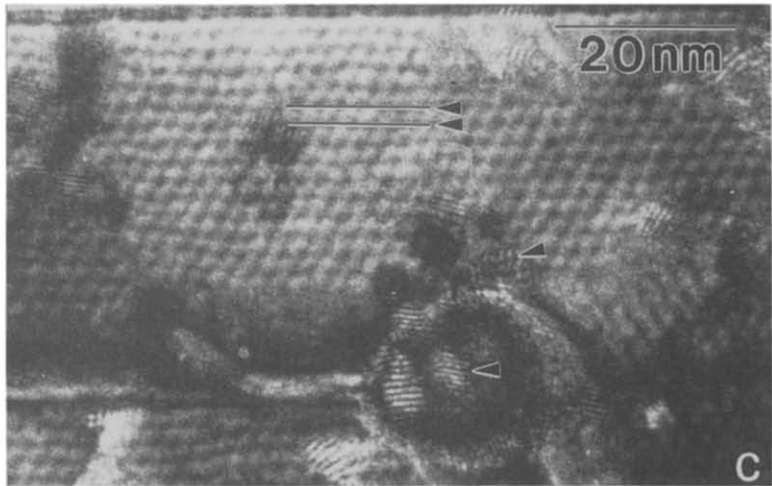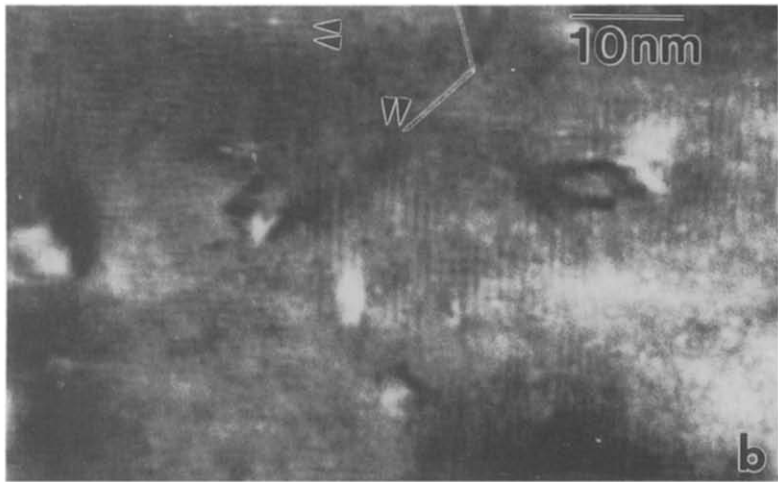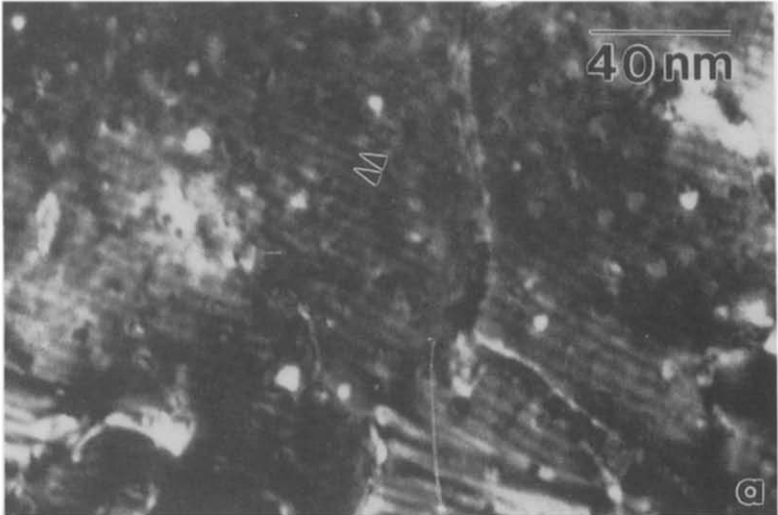


Fig. 5 (continued).

the reconstructed domains. The intensity of diffraction spots decreases, as would be expected off the zone; and the best conditions for imaging are on the zone or in a two-beam condition, as can be seen in fig. 6. It should be noted that there is ample contrast from the surface in all the cases that we have observed to date using conventional microscopy techniques, and it is not necessary to resort to weak-beam techniques to obtain sufficient contrast levels from the surface.

## 6. Discussion

The techniques described herein appear to be applicable to essentially all simple elemental materials. Clearly there may be problems with compounds, and one will probably have to employ annealing in gas environments in order to reestablish stoichiometry. We have demonstrated the feasibility of this approach by oxidizing and reducing a catalyst sample [18] and nickel/nickel oxide in situ using the optical annealing source [19], so this can also be done without destroying specimens.

It is appropriate to point out that there are still some problems with this sort of surface preparation. The sensitivity of PEELS to surface contaminants is not as good as we would like, and one almost certainly needs in situ Auger spectroscopy. This can be done outside the microscope, but there are uncertainties as to the position of Auger electron collection relative to the area imaged in the microscope. The best solution almost certainly requires the Auger spectrometer to be in the microscope. There would also be much to be said for using a FEG source, both in terms of better sensitivity in spectroscopy and for obtaining high-resolution diffraction data from small regimes to avoid domain averaging.

In addition, there are uncertainties as to the temperature at the specimen during annealing. In general, there will be a temperature gradient across most samples due to variations in thickness. We have found optical annealing to be the least palatable choice for two reasons. First, it tends to heat up a large portion of the chamber thereby increasing the probability of contaminating the specimen. In addition, the heating rate during optical annealing is a materials-dependent parameter and varies with the reflectivity of the surface. There are still concerns about the contaminants degassing from the walls of the system, in our case both in the STC and in the microscope.

Finally, although our approach produces samples which are largely defect-free, it will not produce samples with very low defect concentrations. Although this is a disadvantage it is also a real advantage; one area where UHV electron microscopy is likely to make a unique impact is in the interaction of defects with surfaces.

Despite these concerns, it does appear realistic to reproducibly make thin specimens. We should note that the gold sample took about 6 months for us to find the right conditions, but armed with this knowledge we were able to make a suitable silicon specimen in about 3 days.

## 7. Conclusions

Surface-science-grade transmission electron microscopy samples can be produced by ion beam thinning and annealing with sufficient care. The condition of the surface can be monitored by standard microscopy techniques, and surface reconstructions readily detected using either off-zone diffraction patterns or on-zone images.

---

Fig. 6. A montage of two-beam and dark-field images from the reconstructed Au(001) and Si(111) surfaces. (a) An off-the-zone-axis dark-field image of the reconstructed Au(001) surface taken with the bulk (220) spot and satellite spots showing moiré fringes (arrowed) from the reconstructed ($5 \times n$) surface. (b) An on-the-zone-axis dark field image taken with the bulk (200) and surface satellite reflections showing moiré fringes (arrowed) from the "5" dimension of the reconstructed Au(001) $5 \times n$ surface. (c) A zone-axis dark-field image of the metastable boron-doped Si(111) $7 \times 7$ surface showing superlattice fringes from the $7 \times 7$ reconstructed surface and some islands of silicon carbide. The stable surface reconstruction is a $\sqrt{3} \times \sqrt{3}$ R30° structure.

# References

[1] K. Takayanagi and K. Yagi, Trans. Jpn. Inst. Met. 24 (1983) 337.

[2] S. Iijima, Ultramicroscopy 6 (1981) 41.

[3] D. Cherns, Phil. Mag. 30 (1974) 549.

[4] J.P.F. Levitt and A. Howie, J. Microscopy 116 (1979) 89.

[5] K. Kambe and G. Lehmpfuhl, Optik 42 (1975) 187.

[6] K. Takayanagi, Y. Tanishiro, M. Takahashi and S. Takahashi, J. Vac. Sci. Technol. A 3 (1985) 1502.

[7] K. Takayanagi, Y. Tanishiro, M. Takahashi and S. Takahashi, Surf. Sci. 164 (1985) 367.

[8] K.J. Hanson, J.M. Gibson and M.L. McDonald, J. Electrochem. Soc. 136 (1989) 2214.

[9] J.M. Gibson, in: Surface and Interface Characterization, Eds. A. Howie and U. Valdrè (Plenum, New York, 1988) p. 55.

[10] J.M. Gibson, M.Y. Lanzerotti and V. Elser, Appl. Phys. Lett. 55 (1989) 1394.

[11] J.M. Gibson, J.L. Batstone and M.Y. Lanzerotti, in: Evaluation of Advanced Semiconductor Materials by Electron Microscopy, Ed. D. Cherns (Plenum, New York, 1990) p. 295.

[12] G. Nihoul, K. Abdelmoula and J.J. Metois, Ultramicroscopy 12 (1984) 353.

[13] J.C. Heyraud and J.J. Metois, Surf. Sci. 100 (1980) 519.

[14] K. Yagi, K. Takayanagi and G. Honjo, in: Crystals, Growth, Properties and Applications, Vol. 2 (Springer, Berlin, 1982) p. 48.

[15] D.N. Dunn, J.P. Zhang and L.D. Marks, Surf. Sci. 260 (1992), in press.

[16] D.N. Dunn, R. Ai, T.S. Savage, K.L. Merkle and L.D. Marks, Phys. Rev. Lett., submitted.

[17] L.D. Marks, T.S. Savage, J.P. Zhang and R. Ai, Ultramicroscopy 38 (1991) 343.

[18] M. Disko and L.D. Marks, private communication.

[19] M.I. Buckett and L.D. Marks, in preparation.